Journal of ELECTRONIC MATERIALS, Vol. 41, No. 9, 2012
DOI: 10.1007/s11664-012-2165-8

Hyperelastic Property Measurements of Heat-Cured Silicone Adhesives by Cyclic Uniaxial Tensile Test

JUE LI,[1,3] TAPIO TARVAINEN,[1] JAANA RICH,[2] MARKUS TURUNEN,[1] and MERVI PAULASTO-KRÖCKEL[1]

1.—Department of Electronics, Aalto University School of Electrical Engineering, Espoo, Finland. 2.—Department of Biotechnology and Chemical Technology, Aalto University School of Chemical Technology, Espoo, Finland. 3.—e-mail: jue.li@aalto.fi

Most of the commonly used linear elastic properties of silicone adhesives cannot precisely represent their material behavior, knowledge of which is crucial to the reliability study of electronic devices. For this reason, in this paper a widely used silicone adhesive, namely Loctite 5404, is chosen for measuring hyperelastic properties via cyclic uniaxial tensile tests. A special sample preparation procedure is developed to avoid the formation of detrimental air bubbles in the samples. Two maximum strain levels, 20% and 40%, are used in the tests. Each test includes five cyclic loadings to produce a stable stress–strain loop. Three orders of magnitude of strain rate changes are studied, and the stress–strain response of the material is found to be strain rate dependent. The measured stress–strain data are imported into Abaqus finite-element software to calibrate the material coefficients of hyperelastic material models (Mooney–Rivlin, Yeoh, Ogden, and van der Waals models). This is the first time that the hyperelastic properties of the studied silicone adhesive are presented. The determined material coefficients can be used directly in finite-element analyses and thus in reliability studies of electronic devices.

Key words: Silicone adhesive, hyperelastic, air bubbles, finite-element analysis, reliability study

INTRODUCTION

Silicone adhesives are often used as binders in electronic devices for bonding metallic heat sinks, silicon or ceramic chips, circuit board substrates, etc. Linear elastic properties of silicone adhesives cannot precisely represent their material behavior, which is indeed hyperelastic and shows the "Mullins effect."[1] To study the reliability of electronic devices thoroughly, better understanding of the material behavior of silicone adhesives becomes necessary. Therefore, in this study a silicone adhesive, Loctite 5404, is chosen for measuring hyperelastic properties via cyclic uniaxial tensile tests.

Hyperelastic material properties of silicone adhesives are seldom reported in literature. This is mainly due to the fact that the available standard, ASTM D412, is only for tensile strength measurement, and there are no existing test standards for measuring hyperelastic material properties of rubber-like materials.[2] Hyperelastic models are usually described in terms of several material coefficients. With measured stress–strain test data, a curve-fitting procedure is needed to calculate the material coefficients of hyperelastic models. The fitting is normally more accurate if test data from multiple types of tests are available (uniaxial, equibiaxial, pure shear, and volumetric tests). However, using multiple test data sometimes leads to convergence difficulties or unstable material models. This is because rubber-like materials are extremely sensitive to the process of sample preparation. It is a challenge to produce tensile, equibiaxial, or pure shear samples with identical mechanical behaviors, and therefore only uniaxial tensile tests are carried

(Received February 18, 2012; accepted May 26, 2012; published online June 29, 2012)

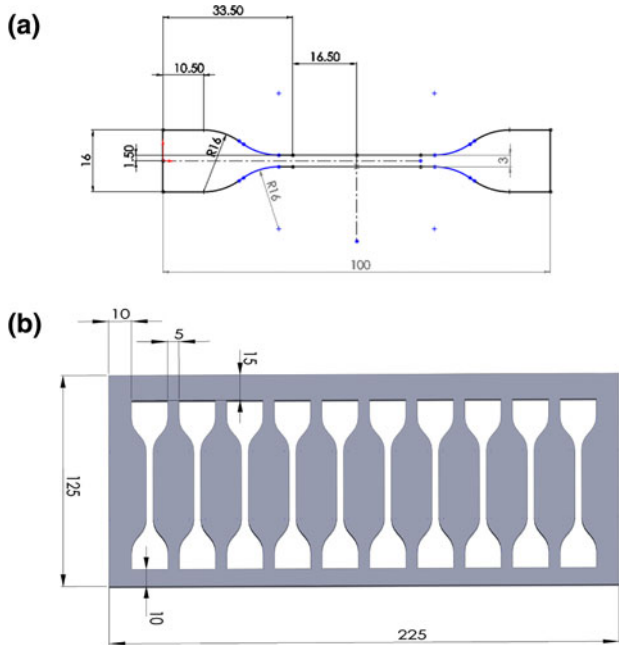

Fig. 1. (a) Dimensions of the tensile sample (in mm) and (b) 2-mm-thick steel plate for the molding of the adhesive.

out in the current study. Furthermore, using samples with large or numerous entrapped air bubbles often leads to early sample failure and erroneous test results. Special sample preparation techniques are necessary to eliminate such detrimental air bubbles.

In the current work, the cyclic uniaxial tensile tests include two maximum strain levels and three orders of strain rate changes in order to study the effect of different strain levels and the strain rate sensitivity. The paper is organized as follows. Firstly, the details of the sample preparation and test setup are reported, followed by a brief introduction of the hyperelastic models. Secondly, the measured stress–strain responses of silicone adhesive are presented and the strain rate sensitivity of the material is studied. Thirdly, the curve-fitting procedure is addressed, and all the calculated material coefficients of the hyperelastic models are reported. Finally, conclusions drawn from the sample preparation, test setup, and test results are given.

MATERIALS AND METHODS

Sample Preparation

The studied commercial silicone adhesive is heat-cured Loctite 5404. Some features of this adhesive are described in the product datasheet.[3] Details of the sample design, mold design, dispensing process, and exicator treatment are presented below.

It is well known that tensile samples should be notably long in relation to their width and thickness for achieving pure tensile strain during tests.[2] Since there are no existing standards for hyperelastic property measurements, a dumbbell sample was designed for the current study (Fig. 1a). All dimensions

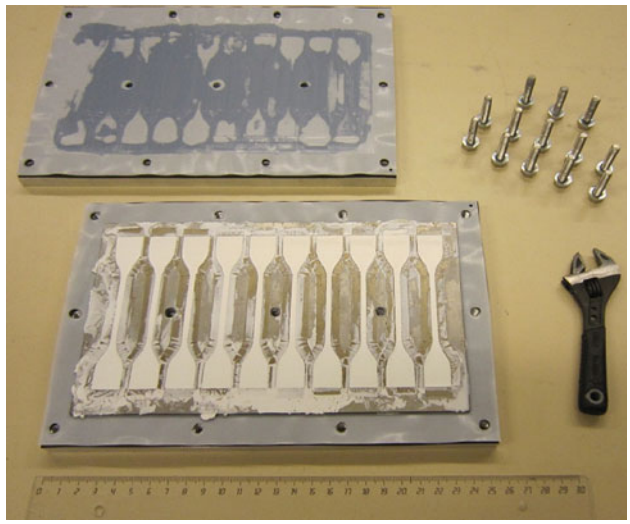

Fig. 2. The opened mold with ten cured samples in the slots. It consists of two 9.5-mm-thick aluminum plates, two 2-mm-thick rubber sheets, two 0.25-mm-thick PTFE sheets, and a 2-mm-thick steel plate.

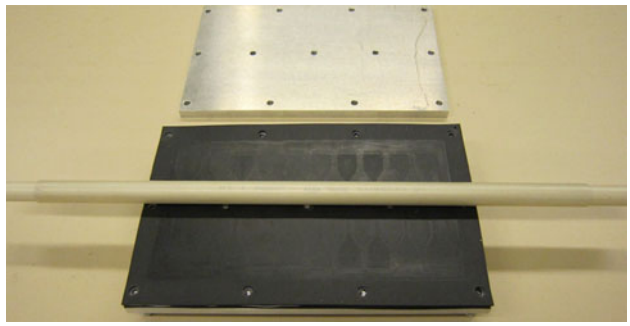

Fig. 3. A plastic tube is rolled from the middle to both sides before closing the mold, in order to press any excess adhesive and air out of the mold slots.

are given in millimeters, and the thickness of the sample is 2 mm in all cases.

Figure 2 shows the opened mold with ten cured samples in the slots. The mold design is similar to a "sandwich structure," consisting of two 9.5-mm-thick aluminum plates, two 2-mm-thick rubber sheets, two 0.25-mm-thick polytetrafluoroethylene (PTFE) sheets, and a 2-mm-thick steel plate (Fig. 1b). The walls of the mold slots are covered with PTFE tapes to ensure that the samples can be easily detached after curing. It is noteworthy that the PTFE tapes cannot be replaced by silicone spray. Experiments show that the latter increases the amount of air bubbles in the samples and fails to completely prevent stiction between the samples and the steel plate.

The volume of one mold slot was about 2 mL, and thereby 20 mL of adhesive was needed to fill all ten slots in the mold. The adhesive was dispensed using an Oki DX-250 digital dispenser. The dispensing pressure should be lower than 3 bar, otherwise air may flow around the piston and increase the size

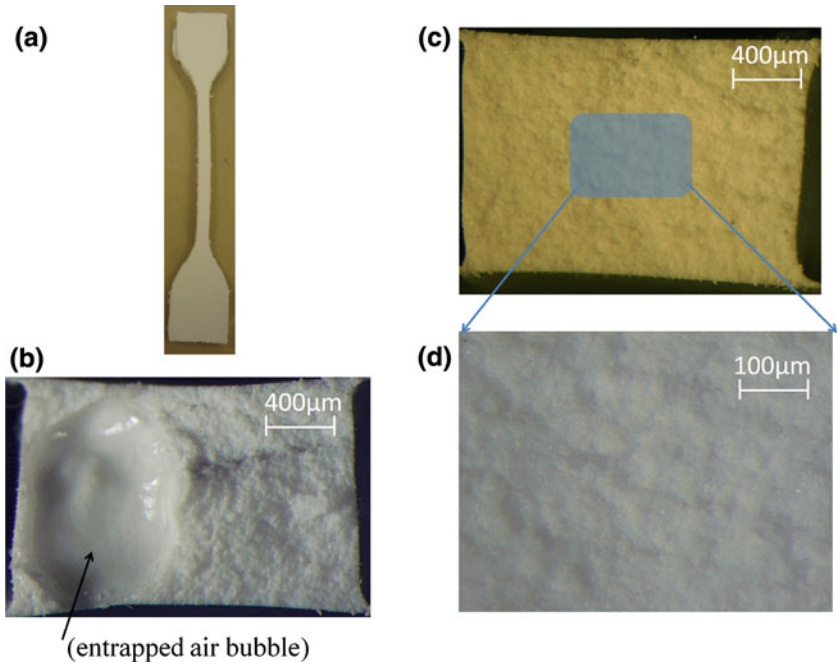

Fig. 4. (a) A qualified tensile sample; (b) cross-section view of a discarded sample with a detrimental air bubble entrapped; (c) cross-section view of a qualified sample after breaking; and (d) enlarged central region of (c), containing no visible air bubbles.

and number of air bubbles in the samples. After dispensing, the opened mold was kept in an exicator for at least 2 h to remove entrapped air bubbles. Before closing the mold, the top PTFE and rubber sheets were placed on top of the steel plate, and then a plastic tube was rolled on the surface of the rubber sheet (from the middle to both sides) to press any excess adhesive and air out of the mold slots (Fig. 3). The heat curing took place in a thermal chamber during 2 h at temperature of 150°C. After curing, the unopened mold was left to cool down at 22°C (room temperature) for approximately 30 min.

Air bubbles are extremely detrimental to the quality of the samples. Using samples with large air bubbles often leads to early sample failure and erroneous test results. After sample preparation, all the samples were carefully checked, and only those without any visible air bubbles were used for tests (Fig. 4a). Furthermore, the cross-sections of the tested samples were also examined by stereomicroscopy (Olympus SZX9). Any test results associated with samples affected by air bubbles were discarded (e.g., Fig. 4b). Figure 4c, d shows the cross-section view of one qualified sample after breaking where no air bubbles or voids are visible.

Test Setup

All the tests were carried out with the help of a mechanical extensometer (INSTRON 33R4204) equipped with a 100-N load cell. The ambient temperature was 22°C, while the relative humidity was set to 50%. Both ends of each sample were clamped by the grips of the test machine. The distance between the grips was 70 mm, and the straight part of the sample was 45 mm long. Since the state of stress and strain was complicated near the sample clamps and the pure tensile strain took place in the straight part of the sample, engineering strain was calculated via $\Delta l/L_0$ (where Δl is the change of length and $L_0 = 45$ mm). The force and engineering strain were recorded at a sampling rate of 10 Hz. Furthermore, the rate of separation of the grips was kept at a certain value: 0.1 mm/s, 1 mm/s, or 8 mm/s (the maximum speed of the machine). The reason for using three different loading rates was to investigate the influence of strain rate on the stress–strain response. Before the cyclic uniaxial tensile tests, three samples were submitted to simple uniaxial tensile tests (i.e., pull-to-failure tests). The maximum elongation of the adhesive was found to be 69%. Besides, the hyperelastic property measurements focused more on the stress–strain behavior in the range of use. According to the application, the strain level of silicone adhesive is usually below 50%. Therefore, two intermediate strain values, i.e., 20% and 40%, were set as the maximum strain levels in the cyclic tests. During each loading cycle, the samples were stretched to the maximum strain level at a certain rate and then returned to the zero-stress state. To obtain a stable stress–strain loop, each sample experienced five cyclic loadings. There were three samples tested under each loading condition.

Hyperelastic Models

According to the continuum mechanics approaches, an isotropic and nearly incompressible hyperelastic

material is usually described in terms of a strain energy potential that depends on one or more of the three strain invariants of the deviatoric Cauchy–Green tensor.[4] There are various forms of strain energy potential available for modeling hyperelastic materials (Ogden form, van der Waals form, Marlow form, Arruda–Boyce form, polynomial form, and its particular cases, e.g., reduced polynomial form, neo-Hookean form, Mooney–Rivlin form, and Yeoh form).[4–8] Some of the popular hyperelastic models are briefly introduced here.

The form of the *polynomial* strain energy potential is

$$U = \sum_{i+j=1}^{N} C_{ij}(\bar{I}_1 - 3)^i(\bar{I}_2 - 3)^j + \sum_{i=1}^{N} \frac{1}{D_i}(J_{el} - 1)^{2i}, \quad (1)$$

where U is the strain energy potential per reference volume, $\bar{I}_1$ and $\bar{I}_2$ are the first and second deviatoric strain invariants, N is the polynomial order, and J_{el} is the elastic volume strain. C_{ij} is the material parameter for shear behavior description, and D_i defines the compressibility of the material, which is set to zero for fully incompressible materials.

If $N = 1$, the two-parameter *Mooney–Rivlin* form of the strain energy potential is obtained as follows:

$$U = C_{10}(\bar{I}_1 - 3) + C_{01}(\bar{I}_2 - 3) + \frac{1}{D_1}(J_{el} - 1)^2. \quad (2)$$

The *reduced polynomial* form is a particular form of the polynomial model. By making the strain energy density irrelevant to the second invariant (setting $j = 0$), the reduced polynomial form is recovered as

$$U = \sum_{i=1}^{N} C_{i0}(\bar{I}_1 - 3)^i + \sum_{i=1}^{N} \frac{1}{D_i}(J_{el} - 1)^{2i}. \quad (3)$$

If $N = 1$, a special form of the reduced polynomial model, namely the *neo-Hookean* form, is obtained as

$$U = C_{10}(\bar{I}_1 - 3) + \frac{1}{D_1}(J_{el} - 1)^2. \quad (4)$$

The *Yeoh* form is a special case of the reduced polynomial form with $N = 3$:

$$U = \sum_{i=1}^{3} C_{i0}(\bar{I}_1 - 3)^i + \sum_{i=1}^{3} \frac{1}{D_i}(J_{el} - 1)^{2i}. \quad (5)$$

The *Ogden* form is expressed in terms of the deviatoric principal stretches, $\bar{\lambda}_i$, as

$$U = \sum_{i=1}^{N} \frac{2\mu_i}{\alpha_i^2}\left(\bar{\lambda}_1^{\alpha_i} + \bar{\lambda}_2^{\alpha_i} + \bar{\lambda}_3^{\alpha_i} - 3\right) + \sum_{i=1}^{N} \frac{1}{D_i}(J_{el} - 1)^{2i}, \quad (6)$$

where μ_i and α_i are material parameters. The *van der Waals* form of potential, also known as the Kilian model, is

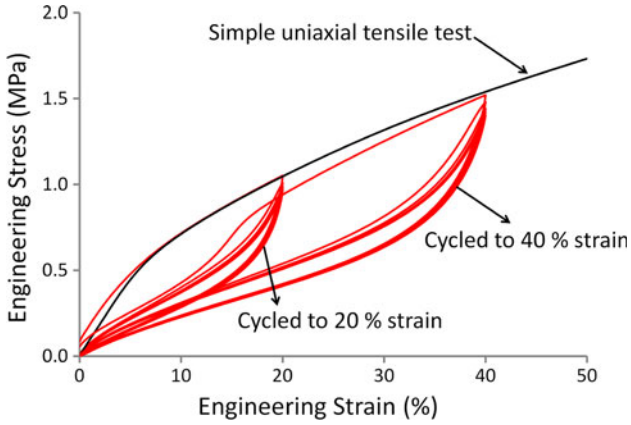

Fig. 5. Stress–strain data of the silicone adhesive samples subjected to a simple uniaxial tensile test and cyclic uniaxial tensile tests.

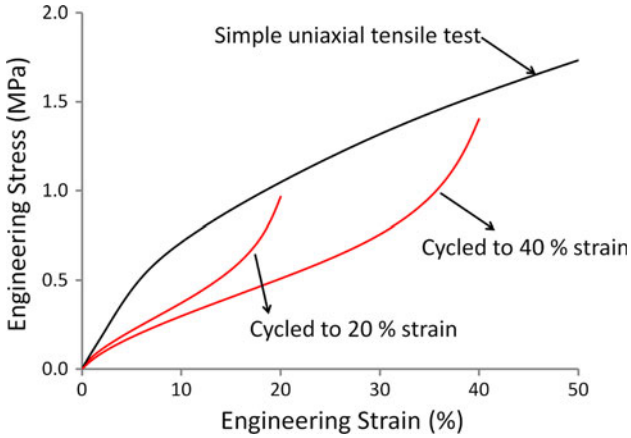

Fig. 6. Stress–strain curve of a simple uniaxial tensile test and the stabilized curves of the cyclic uniaxial tensile tests.

$$U = \mu\left\{-(\lambda_m^2 - 3)[\ln(1-\eta) + \eta] - \frac{2}{3}\alpha\left(\frac{\tilde{I} - 3}{2}\right)^{\frac{3}{2}}\right\} + \frac{1}{D}\left(\frac{J_{el}^2 - 1}{2} - \ln J_{el}\right), \quad (7)$$

where $\tilde{I} = (1-\beta)\bar{I}_1 + \beta\bar{I}_2$ and $\eta = \sqrt{(\tilde{I} - 3)(\lambda_m^2 - 3)}$. μ is the initial shear modulus, λ_m is the locking stretch, α is the global interaction parameter, and β is an invariant mixture parameter.

The form of the *Marlow* strain energy potential is

$$U = U_{dev}(\bar{I}_1) + U_{vol}(J_{el}), \quad (8)$$

where U_{dev} and U_{vol} are the deviatoric part and volumetric part of U.

As presented above, there are many options for modeling a hyperelastic material. The choice of the most suitable hyperelastic model depends on the application and available test data. The Ogden and van der Waals forms are more accurate in fitting experimental data from multiple types of tests

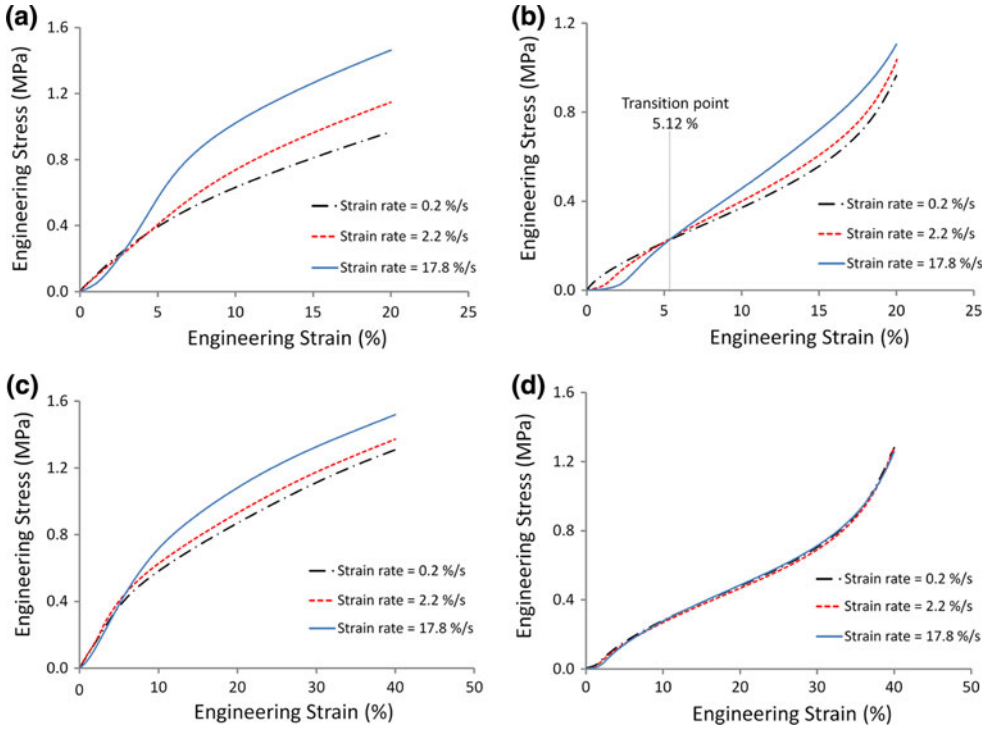

Fig. 7. Stress–strain curves with different strain rates from (a) the first load under 20% maximum strain level, (b) the fifth load (stabilized) under 20% maximum strain level, (c) the first load under 40% maximum strain level, and (d) the fifth load (stabilized) under 40% maximum strain level.

(uniaxial, equibiaxial, pure shear, and volumetric tests). The van der Waals, Yeoh, and reduced polynomial forms provide acceptable results if limited test data are available for data fitting. The Marlow form gives the best fitting results when only one type of test data is available. However, the Marlow form does not have any material coefficients, and it can only be defined by the test data, which is relatively inconvenient. The choice of the right order of N is commonly related to the maximum strain level; For example, $N = 1$ for the polynomial form and $N = 2$ for the Ogden form if the maximum strain level is less than 100%. A thorough comparison of all the hyperelastic models lies outside the scope of this study. More details of the subject can be found in the Refs. 9–11.

RESULTS AND DISCUSSION

Stress–Strain Responses

Figure 5 presents the stress–strain responses of the samples subjected to the simple uniaxial tensile test and cyclic uniaxial tensile tests. The behavior of the studied silicone adhesive is similar to other rubber-like materials that commonly exhibit the Mullins effect. As shown in Fig. 5, there is an obvious stress softening after the first load, and the softening takes place whenever the loading is lower than or equal to the maximum strain level. When the extension exceeds the previously applied maximum strain level, the stress–strain curve returns to the curve of the simple uniaxial tensile test. It has been found that five loading cycles are enough to obtain a stable stress–strain loop of the material.

Before fitting the hyperelastic material models, one needs to make a choice between different stress–strain situations. As shown in Fig. 6, the stress–strain responses of the same material can change significantly between two different loading stages: the first load of a virgin material and the fifth load (stabilized curve) during the cyclic test. The material properties extracted from a loading condition should only be applied to the associated application, otherwise unpredictable errors may be introduced; For instance, if the behavior of a virgin material is expected, the test data of the simple uniaxial tensile test is appropriate. If the material in the stabilized state is of interest, the stabilized curve of a cyclic test is significant. Moreover, if one is interested in the overall response of the material, such as the loading and unloading cycles shown in Fig. 5, data including multiple loading and unloading cycles are necessary, and the damage of the material needs to be considered in the material model, e.g., the Mullins effect model in Abaqus.

Strain Rate Sensitivity

Electronic materials usually experience a relatively large strain rate range depending on the application; For instance, the strain rate of a printed wiring board during thermal cycling is around 0.1%/s, while the strain rate during a shock impact

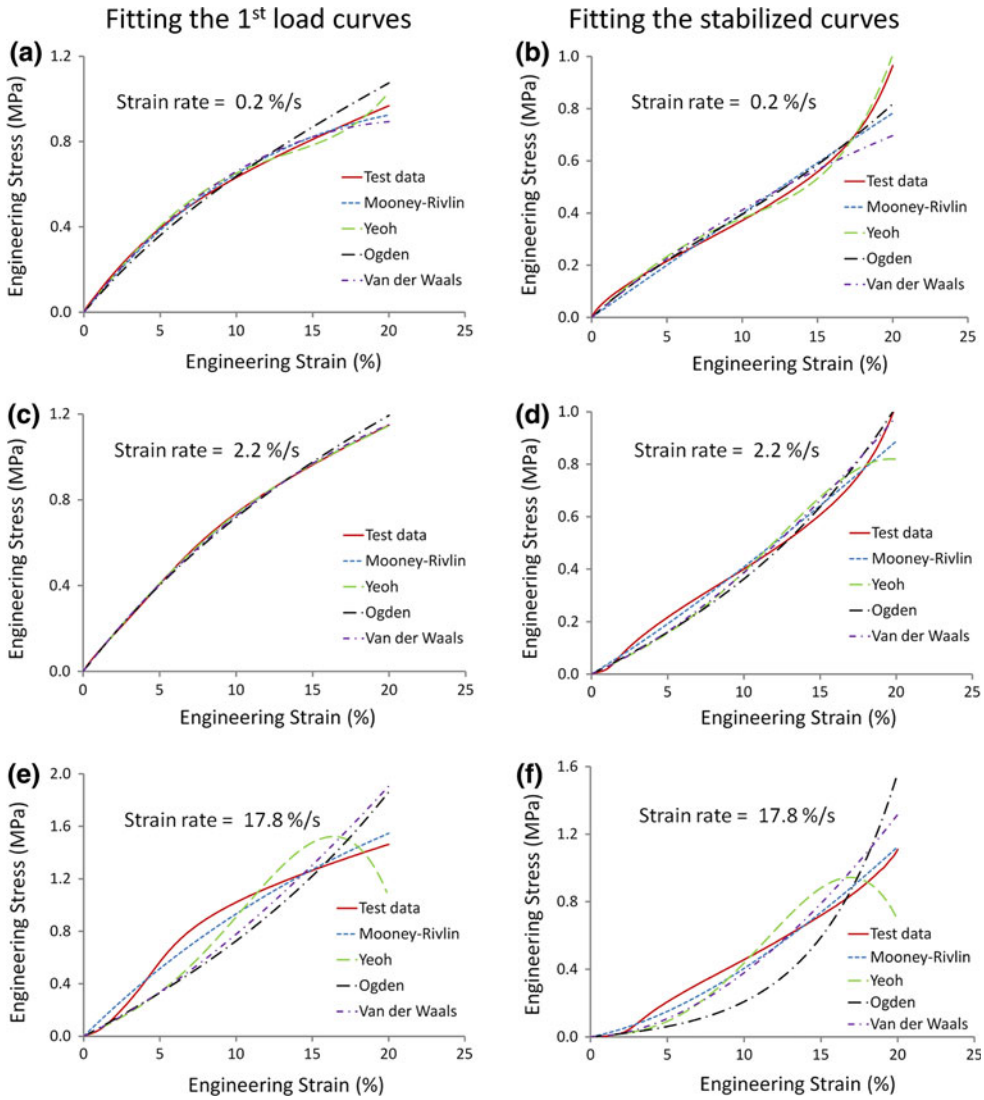

Fig. 8. Curve fitting with uniaxial test data and 20% maximum strain level: (a) fitting the first load curves with the 0.2%/s strain rate, (b) fitting the stabilized curves with the 0.2%/s strain rate, (c) fitting the first load curves with the 2.2%/s strain rate, (d) fitting the stabilized curves with the 2.2%/s strain rate, (e) fitting the first load curves with the 17.8%/s strain rate, and (f) fitting the stabilized curves with the 17.8%/s strain rate.

can be 100%/s or even higher. Understanding the strain rate-dependent material responses is crucial to successful reliability study of electronic products. Figure 7 presents the initial and stabilized stress–strain responses from two maximum strain levels and three different strain rate levels that cover three orders of strain rate changes. The strain rate dependency is visible in all cases except for the stabilized curves under 40% maximum strain level (Fig. 7d). By comparing Fig. 7a, b with Fig. 7c, d, it is found that the material is more strain rate dependent when the maximum strain level is lower. In general, the material exhibits strain rate hardening for the first time loading or when subjected to a low maximum strain level. However, Fig. 7b shows the transition from strain rate softening to strain rate hardening with increasing strain values. In Fig. 7b the three curves nearly intersect at one point (about 5.12% strain). The mechanism behind this phenomenon is still unclear. One possible explanation could be that after the 5.12% strain the chains are mostly oriented and ready to slide in relation to each other. With higher strain rate, the friction is larger and thus leads to the strain rate hardening shown in Fig. 7b.

Curve-Fitting Procedures

The measured test data were imported into the finite-element software Abaqus 6.9-EF to calculate the material coefficients of the hyperelastic material models. Abaqus determines the material coefficients via a least-squares fitting procedure (linear least-squares fit for the polynomial and reduced polynomial forms, and nonlinear least-squares fit for the Ogden, Arruda–Boyce, and van der Waals forms). Since the maximum strain level in the current study is relatively low (less than 50%), the following four

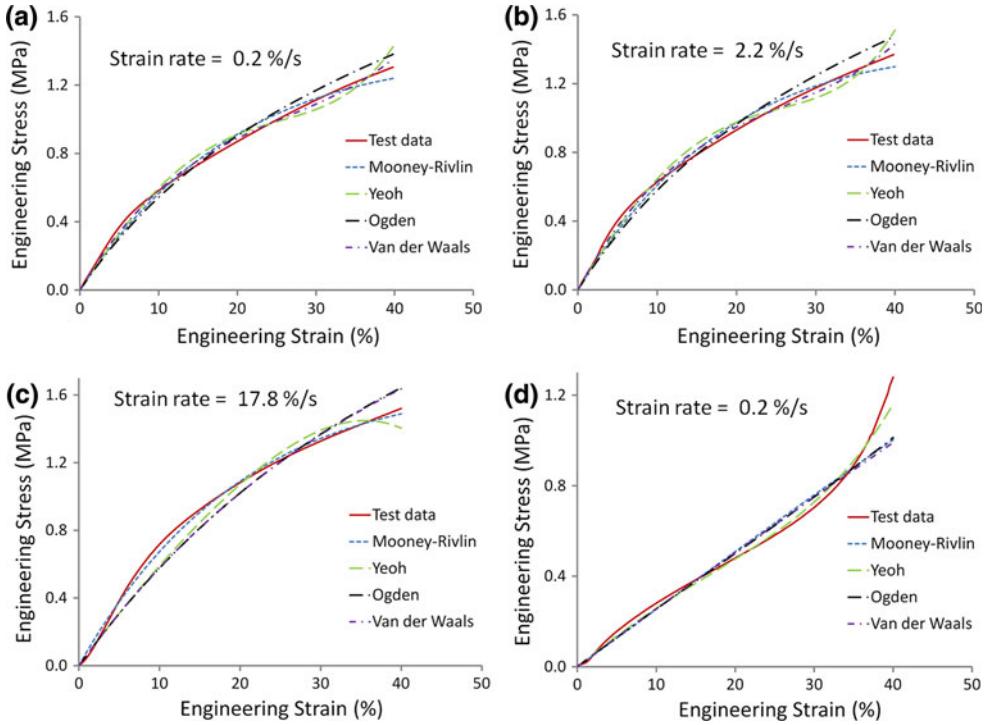

Fig. 9. Curve fitting with uniaxial test data and 40% maximum strain level: (a) fitting the first load curves with the strain rate of 0.2%/s, (b) fitting the first load curves with the strain rate of 2.2%/s, (c) fitting the first load curves with the strain rate of 17.8%/s, and (d) fitting the stabilized curves with the strain rate of 0.2%/s.

Table I. Material coefficients of Mooney–Rivlin model

Loading Conditions	Strain Rate (%/s)	C_{10}	C_{01}
First load curves with 20% maximum strain level	0.2	−2.076	3.589
	2.2	−1.004	2.566
	17.8	−0.406	2.323
Stabilized curves with 20% maximum strain level	0.2	1.281	−0.608
	2.2	2.325	−1.737
	17.8	5.202	−4.907
First load curves with 40% maximum strain level	0.2	−0.532	1.721
	2.2	−0.668	1.957
	17.8	−0.612	2.029
Stabilized curve with 40% maximum strain level	0.2	0.925	−0.506

Table II. Material coefficients of Yeoh model

Loading Conditions	Strain Rate (%/s)	C_{10}	C_{20}	C_{30}
First load curves with 20% maximum strain level	0.2	1.504	−6.676	27.582
	2.2	1.470	−2.522	5.909
	17.8	–	–	–
Stabilized curves with 20% maximum strain level	0.2	0.879	−4.653	32.514
	2.2	0.473	5.193	−22.594
	17.8	–	–	–
First load curves with 40% maximum strain level	0.2	1.177	−1.607	1.943
	2.2	1.276	−1.808	2.159
	17.8	–	–	–
Stabilized curve with 40% maximum strain level	0.2	0.478	−0.128	0.605

forms of strain energy potential were selected for fitting the uniaxial tensile test data:

1. The Mooney–Rivlin form (the polynomial form with $N = 1$)
2. The Yeoh form (the reduced polynomial form with $N = 3$)
3. The Ogden form with $N = 1$
4. The van der Waals form

Figure 8 compares the predicted response curves of different strain energy potentials with the experimental data with 20% maximum strain level. Figure 9a, c, e shows curve-fitting results of the first load test data with different strain rate, while Fig. 9b, d, f shows the stabilized curves. Throughout all six cases shown in the figure, the Mooney–Rivlin form gives, generally, the best predictions. The performance of the Ogden and van der Waals forms is acceptable as well. The Yeoh form successfully predicts the upturn tendency in Fig. 8b, but it shows unstable behavior in the cases with high strain rate (Figs. 8e, f). The fitting results of the test data with the 17.8%/s strain rate are not

Table III. Material coefficients of Ogden model ($N = 1$)

Loading Conditions	Strain Rate (%/s)	μ_1	α_1
First load curves with 20% maximum strain level	0.2	2.802	−7.674
	2.2	3.049	−5.067
	17.8	2.096	9.156
Stabilized curves with 20% maximum strain level	0.2	1.803	−16.786
	2.2	0.983	10.713
	17.8	0.293	23.752
First load curves with 40% maximum strain level	0.2	2.283	−4.398
	2.2	2.431	−4.355
	17.8	2.197	0.420
Stabilized curve with 40% maximum strain level	0.2	0.887	3.739

Table IV. Material coefficients of van der Waals model

Loading Conditions	Strain Rate (%/s)	μ	λ	a	β
First load curves with 20% maximum strain level	0.2	3.101	10.008	20.10	0.0
	2.2	3.048	10.023	1.243	0.0
	17.8	1.868	73.264	−4.388	0.0
Stabilized curves with 20% maximum strain level	0.2	1.660	9.989	0.352	0.781
	2.2	0.856	10.016	−5.345	0.0
	17.8	0.104	22.204	−103.802	0.0
First load curves with 40% maximum strain level	0.2	2.635	2.234	2.746	0.0
	2.2	2.886	2.221	2.847	0.0
	17.8	–	–	–	–
Stabilized curve with 40% maximum strain level	0.2	0.875	9.962	−0.466	0.0

satisfactory. This is mainly due to the strain rate softening taking place at the low strain range (Fig. 7b). If one is not interested in the strain rate softening or only expects moderate or high strains, deleting some data points at the low strain range may significantly improve the curve-fitting performance.

Figure 9 presents the predicted response curves of different strain energy potentials for the experimental data with the 40% maximum strain level. Since the stabilized stress–strain curve under the 40% maximum strain level is not sensitive to the strain rate (Fig. 7d), it is sufficient to use one curve with 0.2%/s strain rate for the curve fitting (Fig. 9d). Again, the Yeoh form captures the S-shaped feature of the stabilized stress–strain curve with the 40% maximum strain level, but its predictions for the first load curves are poor. The Mooney–Rivlin, Ogden, and van der Waals forms give acceptable predictions for the first load curves, although they fail to capture the S-shape of the stabilized curve. All the material coefficients are presented in Tables I–IV, each table including the coefficients of one certain hyperelastic model. Those coefficients associated with the unstable models are not listed.

CONCLUSION

In this work, the hyperelastic material properties of Loctite 5404 silicone adhesive were studied by cyclic uniaxial tensile tests. Special tools and procedures for sample preparation were developed to eliminate the detrimental entrapped bubbles from the samples. In total, two maximum strain levels (20% and 40%) and three different strain rate levels (0.2%/s, 2.2%/s, and 17.8%/s) were investigated. Except for the stabilized curves with a 40% maximum strain level, the stress–strain responses of the material are strain rate dependent. Moreover, based on the curve-fitting procedures, the material coefficients of four forms of strain energy potential (Mooney–Rivlin, Yeoh, Ogden, and van der Waals models) are reported. The Mooney–Rivlin model gives, in general, the best predictions, while the performance of the Ogden and van der Waals models is acceptable. The Yeoh model successfully predicts the upturn tendency of the stabilized stress–strain curves, but it often becomes unstable when the strain rate becomes high. The reported hyperelastic material properties can be directly used in finite-element analyses and benefit reliability studies of electronic devices significantly.

ACKNOWLEDGEMENTS

The authors would like to thank Sini Niiranen for her help in sample preparation. VTI Technologies is gratefully acknowledged for support.

REFERENCES

1. L. Mullins, *Rubber Chem. Technol.* 42, 339 (1969). doi:10.5254/1.3539210.
2. ASTM D412, Standard Test Methods for Vulcanized Rubber and Thermoplastic Elastomers—Tension.
3. Loctite 5404 data sheet, www.szhantech.com/download/upload/shop/w200572590214.pdf.
4. M.C. Boyce and E.M. Arruda, *Rubber Chem. Technol.* 73, 504 (2000). doi:10.5254/1.3547602.
5. M. Mooney, *J. Appl. Phys.* 11, 582 (1940). doi:10.1063/1.1712836.
6. R.S. Rivlin, *Philos. Trans. R. Soc. Lond. A* 241, 379 (1948). doi:10.1098/rsta.1948.0024.
7. R.W. Ogden, *Proc. R. Soc. Lond. A* 326, 565 (1972). doi:10.1098/rspa.1972.0026.
8. O.H. Yeoh, *Rubber Chem. Technol.* 66, 754 (1993). doi:10.5254/1.3538343.
9. M. Levinson and I.W. Burgess, *Int. J. Mech. Sci.* 13, 563 (1971). doi:10.1016/0020-7403(71)90042-7.
10. G. Markmann and E. Verron, *Rubber Chem. Technol.* 79, 835 (2006). doi:10.5254/1.3547969.
11. A. Ali, M. Hosseini, and B.B. Sahari, *J. Sci. Ind. Res. India* 69, 495 (2010).